Cuff Tear Arthropathy with Bone Loss (Acetabular Acromion)

47

Giuseppe Milano, Maristella F. Saccomanno, and Andrea Grasso

47.1 Introduction

The cuff tear arthropathy (CTA) was first described by Neer in the early 1980s [1] as "degenerative changes of the glenohumeral joint consequent to a massive rotator cuff tear" and further defined by Jensen in 1999 [2] as a disease characterized by three main findings: (a) massive rotator cuff tear associated with shoulder pain, muscle atrophy, and loss of motion; (b) degenerative changes in the glenohumeral joint; and (c) upward migration of the humeral head observable on X-rays in anteroposterior (AP) view.

Subsequent radiological classification aimed to define and correlate progressive stages of the disease and consequent treatment strategies [3, 4].

Interestingly, management of CTA has largely changed in the last decades in a way that probably nothing else did in orthopedics. At present, improved arthroscopic techniques and emerging technologies, such as superior capsule reconstruction, may provide a possible treatment solution for certain stages [5]. However, when degenerative changes and bone loss occur, reverse shoulder arthroplasty (RSA) does remain the best treatment option. As imaging tools, design and biomechanical rationale of RSA, and surgical techniques improved, there have been expanding options in augmentation techniques and baseplate fixation, which widens the opportunity to improve the functional outcomes even in the late stages of CTA.

The aim of the present chapter is to provide an overview on pathology, classification, and treatment of CTA with bone loss.

47.2 Pathogenesis

From an epidemiological standpoint, CTA has been reported to be more common in women, in the 6th–7th decades, particularly involving the dominant shoulder [6]. Several risk factors have been identified: rotator cuff tear, rheumatoid arthritis, crystalline-induced arthropathy, and hemorrhagic shoulder (hemophiliacs/anticoagulants) [6]. Recently, Gumina et al. [7], based on the assumption that the instability consequent to massive cuff tear may worsen in patients with joint laxity and that joint laxity is notoriously more common in women, hypothesized that generalized joint laxity could be a risk factor for development of CTA. However, the authors finally showed no correlation at all between joint laxity and glenohumeral osteoarthritis.

G. Milano (✉)
Department of Orthopaedics, University of Brescia, Brescia, Italy
e-mail: giuseppe.milano@unicatt.it

M. F. Saccomanno
Department of Orthopaedics, IRCCS Fondazione Policinico Universitario A. Gemelli, Catholic University, Rome, Italy

A. Grasso
Orthopaedic Unit, Villa Valeria Clinic, Rome, Italy

A. B. Imhoff, F. H. Savoie III (eds.), *Rotator Cuff Across the Life Span*,
https://doi.org/10.1007/978-3-662-58729-4_47

Two main etiopathogenetic theories for CTA have been developed: (a) crystal-mediated and (b) rotator cuff tear-mediated.

In 1981, Halverson et al. [8] proposed a crystal-mediated theory at the origin of CTA. They coined the term "Milwaukee shoulder syndrome" and hypothesized that the trigger point was an immunologic cascade activated by calcium phosphate-containing crystals in the synovial tissue. Subsequently, McCarty et al. [9] showed that basic calcium phosphate crystal accumulation in the glenohumeral joint actually correlates with rotator cuff deficiency. Synovial cells phagocytize the crystals, releasing prostaglandins and proteases that destroy articular cartilage. A positive feedback cycle accelerates degeneration of the rotator cuff and biceps tendon, leading to glenohumeral joint degradation.

On the opposite, Neer et al. [1] hypothesized the rotator cuff theory, which involves both mechanical and nutritional factors. Rotator cuff tears are thought to produce at least two simultaneous negative effects:

- A muscle unbalance that, based on the force couple theory explained later on by Burkhart et al. [10], leads to the upward migration of the humeral head and consequently to glenoid and acromial wear as well as eccentric humeral head motion and premature wear of the articular cartilage in the areas of higher glenohumeral compression.
- Loss of the watertight effect (loss of negative pressure normally existing inside the glenohumeral joint), which allows extravasation of the synovial fluid and, consequently, leads to an impaired delivery of nutrients to the articular surface, so the cartilage is poorly nourished and would easily become atrophied.

Furthermore, pain associated with cuff tear and degenerative changes makes the shoulder range of motion (ROM) rather limited, leading by time to disuse osteoporosis and collapse of the subchondral bone of the humeral head.

47.3 Clinical Features

Patients with CTA are typically elderly and usually describe classical symptoms and functional impairment related both to osteoarthritis and cuff disease. They have a history of progressively worsening pain, accompanied by limited shoulder motion and stiffness. These symptoms may be precipitated by an acute, traumatic event. Patients with a diagnosis of rheumatoid arthritis or of another inflammatory arthropathy may also present with polyarthralgia and a prior history of medical treatment for their systemic disease [11].

The physical examination always starts with a global inspection of both shoulders. Any difference between shoulders in muscle atrophy should be noticed. Swelling and clinical evidence of anterosuperior escape of the humeral head are not uncommon and indicate a gross deficiency of subscapularis and supraspinatus tendons.

Both active and passive ROM are usually very limited by weakness, pain, and stiffness, but at varying degrees. Tests for evaluation of cuff integrity are positive both for pain and strength deficit.

Cervical spine disorders as well as complete deltoid deficiency and any sign of neurological disorders must be ruled out.

47.4 Imaging

Diagnosis of CTA is essentially clinical and radiographic, as standard X-rays in the AP and axillary views may demonstrate characteristic findings. Magnetic resonance (MR) could be helpful in evaluation of cuff tendons and muscle status. A computed tomography (CT) scan is mandatory for preoperative planning especially in the setting of bone loss.

47.4.1 X-Rays

A true AP and axillary views are enough. No specific views are required either for CTA diagnosis or for preoperative planning.

Pathognomonic radiographic signs of CTA are:

- Superior migration of the humeral head, represented by decreased acromiohumeral distance.
- Femoralization of the humeral head, which means erosion of the greater tuberosity.
- Acetabularization of the acromion, represented by a thinning of the coracoacromial arch and superior glenoid erosion.
- Posterior glenoid erosion.
- Glenohumeral subluxation as a result of rotator cuff insufficiency.
- Osteopenia in both the proximal aspect of the humerus and the glenoid.

Joint space narrowing and osteophytes are common findings in CTA as well as in primary osteoarthritis (Fig. 47.1).

CTA has been classified on radiographic imaging according to Hamada [3] and Seebauer [4].

Fig. 47.1 Anteroposterior X-ray view of a right shoulder with some pathognomonic radiographic signs of cuff tear arthropathy (CTA)

The Hamada classification [3] (Fig. 47.2) depicts the process of progressive superior migration of the humeral head:

- Stage 1: the acromiohumeral interval is >6 mm.
- Stage 2: the acromiohumeral interval is <5 mm.
- Stage 3: the acromiohumeral interval is <5 mm, and acetabulization of the coracoacromial arch is present.
- Stage 4: the glenohumeral joint is narrowed, either without acetabulization (Stage 4a) or with acetabulization (Stage 4b).
- Stage 5: humeral head osteonecrosis results in collapse.

The Seebauer classification [4] is quite more complicated and therefore less widespread in clinical practice. It is a biomechanical description of CTA, in which each type is distinguished according to the amount of upward migration of the humeral head from the center of rotation and the amount of instability. The amount of decentralization seen on radiographs is dependent on "the extent of the rotator cuff tear, the integrity of the coracoacromial arch, and the degree and direction of the glenoid bone erosion" [4].

Plain radiographs have also been employed as a tool for preoperative planning. Several classifications have been proposed to assess glenoid wear [12–15]. As a matter of fact, it is important to highlight that bone loss is always multiplanar; therefore, assessing glenoid wear means a comprehensive evaluation of glenoid version [12], inclination [13, 14], and medialization [15]. Glenoid version is usually evaluated on axillary view, whereas inclination can be evaluated on a true AP view, and medialization has been classified on AP and axial views.

Nyffeler et al. [12], after comparing measurement of glenoid version on X-rays and CT scans, actually showed that glenoid retroversion can be overestimated on X-rays in up to 86% of cases; therefore, up to now CT scan is the modality of choice for the estimate of glenoid version.

On the contrary, radiographic classification systems for glenoid inclination and medialization are still valid.

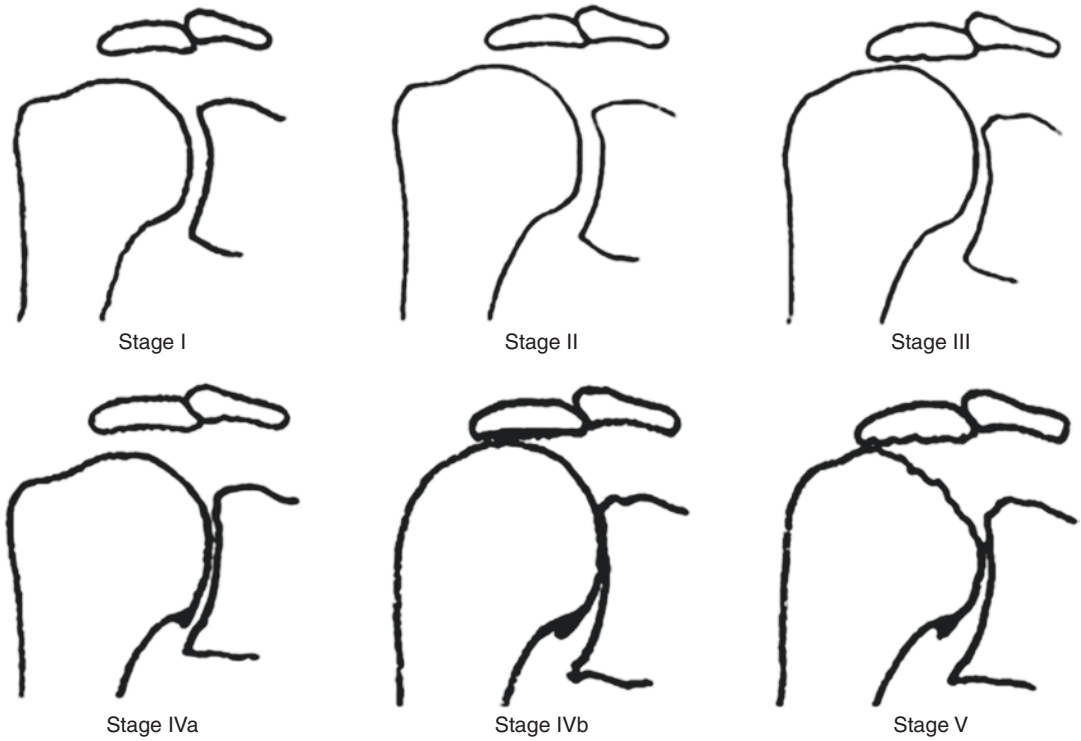

Fig. 47.2 Radiographic classification of CTA according to Hamada [2]

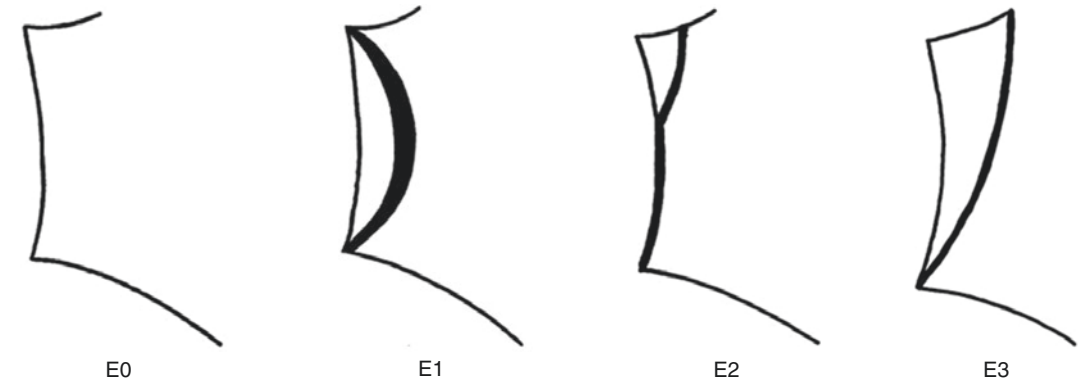

Fig. 47.3 Radiographic classification of glenoid tilt in the coronal plane according to Sirveaux et al. [14]

Anatomically, the angle of inclination of the glenoid is equivalent to the amount of glenoid tilt in the coronal plane and defines the position of the humeral head relative to the subacromial space. The normal glenoid tilt in the coronal plane has been reported to range from −8° to 15.8° (average, 4–5°) [16]. Two classification systems are available [13, 14].

Sirveaux et al. [14] (Fig. 47.3) defined four types of glenoid in order to describe the progression of superior erosion:

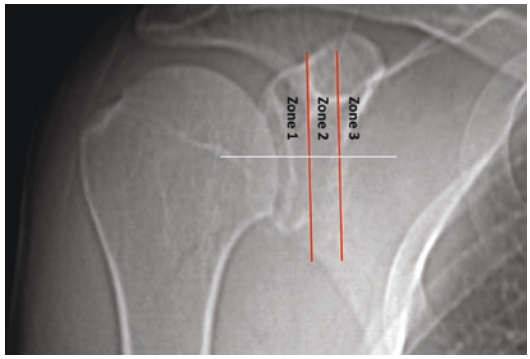

Fig. 47.4 Radiographic classification of glenoid medialization according to Kocsis et al. [15]

- Type E0: the head of the humerus migrated upward without erosion of the glenoid.
- Type E1: concentric erosion of the glenoid.
- Type E2: erosion of the superior part of the glenoid.
- Type E3: erosion extended to the inferior part of the glenoid.

Conversely, Habermeyer et al. [13] depicted the evolution of eccentric inferior glenoid wear. The glenoid inclination angle was measured with the use of one line drawn along the superior and inferior glenoid rim (the glenoid line) and another line drawn along the lateral base of the coracoid process (the coracoid base line) from the superior glenoid rim perpendicular to the bottom margin of the radiograph. Four types of glenoid were identified:

- Type 0: normal glenoid, the coracoid baseline and the glenoid line run parallel.
- Type 1: the coracoid base line and the glenoid line intersect below the inferior glenoid rim.
- Type 2: the coracoid base line and the glenoid line intersect between the inferior glenoid rim and the center of the glenoid.
- Type 3: the coracoid baseline and the glenoid line intersect above the coracoid base.

Very high interobserver reliability was found by the authors [13].

Classification of glenoid medialization has been recently described by Kocsis et al. [15] on AP and axial views. Two anatomical reference points were used to define limits of three zones: the most medial point of the spinoglenoid notch and the most lateral edge of the base of the coracoid (Fig. 47.4). Three types have been recognized:

- Type 1: the most medial (or lowest) point of the intact glenoid articular surface is at the level of or lateral to the base of the coracoid (zone 1).
- Type 2: the most medial (or lowest) point of the intact glenoid articular surface falls between the base of the coracoid and the most medial point of the spinoglenoid notch (zone 2).
- Type 3: the most medial (or lowest) point of the glenoid articular surface reaches the level of the spinoglenoid notch or is medial to it (zone 3).

Excellent inter-method reliability, interobserver reliability, and test-retest reliability were reported by the authors [15].

47.4.2 Magnetic Resonance

Although not essential for diagnosis, MR is useful for assessing the extension of the rotator cuff tear and, even more, muscle atrophy and fatty infiltration (Fig. 47.5). Recent studies showed that degree of rotator cuff muscle fatty infiltration is associated with glenoid type [17]. Moreover, Donohue et al. [18] showed that high-grade fatty infiltration of rotator cuff muscle is associated with increased pathologic glenoid retroversion and increased joint-line medialization.

47.4.3 Computed Tomography

CT scan evaluation is paramount for the preoperative planning. It provides accurate visualization and quantification of glenoid bone stock as well as detecting competence of the coracoacromial arch and/or eventual presence of an acromial stress fracture.

As already mentioned, CT scan is up to now considered the gold standard for definition of glenoid version. Unfortunately, assumptions about how much of the measured glenoid version are

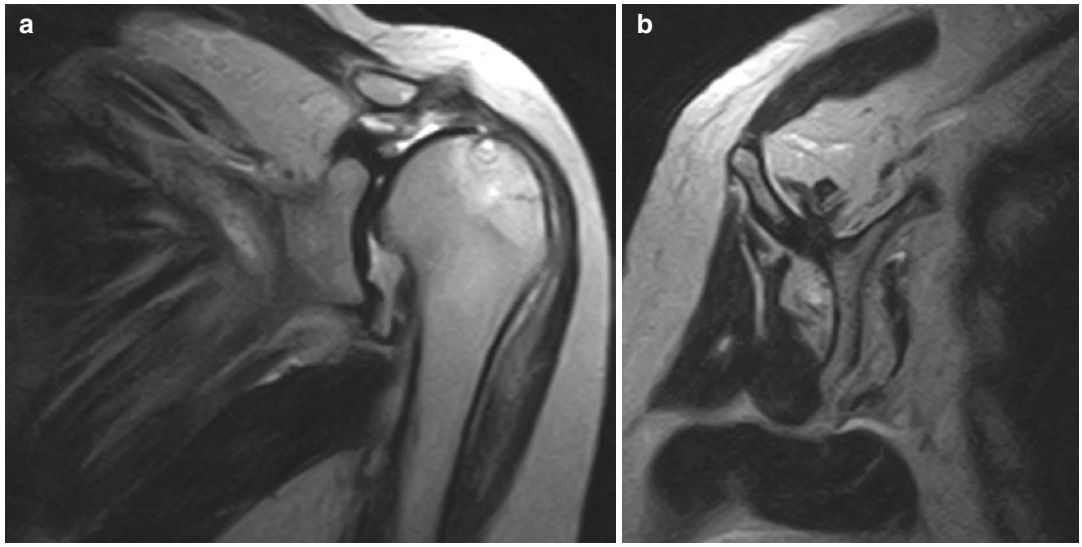

Fig. 47.5 MR is useful for assessing the extension of the rotator cuff tear (**a**) and, even more, muscle atrophy and fatty infiltration (**b**)

physiologic, and how much is pathologic in any one patient is quite complicated due to the fact that native glenoid version has been reported to vary over a 25° range from −14° (retroversion) to +12° (anteversion) [16, 19].

Walch et al. [20] first developed a classification system to describe glenoid version in cases of primary glenohumeral osteoarthritis by using two-dimensional (2D) CT scan. It includes five categories of glenoid patterns:

- A1: centered humeral head, minor erosion.
- A2: centered humeral head, major central glenoid erosion.
- B1: posterior subluxated head, no bony erosion.
- B2: posterior subluxated head, posterior erosion with biconcavity of the glenoid.
- C: dysplastic glenoid with at least 25° of retroversion regardless of erosion.

Recently, the original Walch's classification system was modified by adding new glenoid subtypes [21, 22]. Bercik et al. [21] added the following subtypes (Fig. 47.6):

- B3: monoconcave glenoid and posteriorly worn, with at least 15° of retroversion or at least 70% posterior humeral head subluxation, or both.
- D: glenoid with any level of anteversion or with humeral head subluxation of less than 40% (i.e., anterior subluxation).
- A more precise definition of the A2 glenoid: "cupula" describes a glenoid in which a line drawn from the anterior to posterior rims of the native glenoid transects the humeral head.

Intra- and interobserver reliability were also successfully proved [21].

Davis et al. [22] described the C2 glenoid: a glenoid with greater than 25% of retroversion in addition to posterior subluxation of the humeral head with respect to the glenoid face (Fig. 47.7).

In both studies, glenoid were evaluated by using three-dimensional (3D) CT scan reconstructions. It has been proven that 3D CT reconstructions portray glenoid version more reliably than 2D CT because 3D reconstructions allow reorientation of the scapula as a free body [19, 23–26] (Fig. 47.8).

Advancement in 3D CT reconstruction software and awareness of the wide range of anatomic variations in glenoid version led to define a new 3D glenoid vault model [27]. The internal architecture of the glenoid vault was found

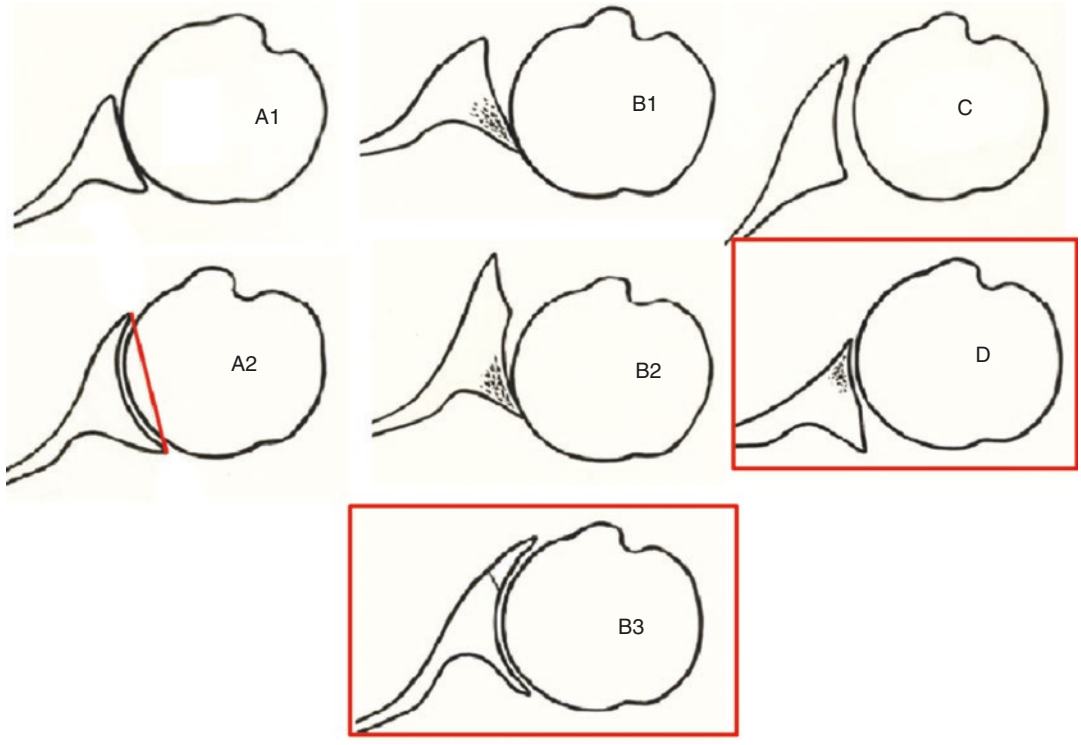

Fig. 47.6 Classification of glenoid version according to Walch et al. [20] modified by Bercik et al. [21]

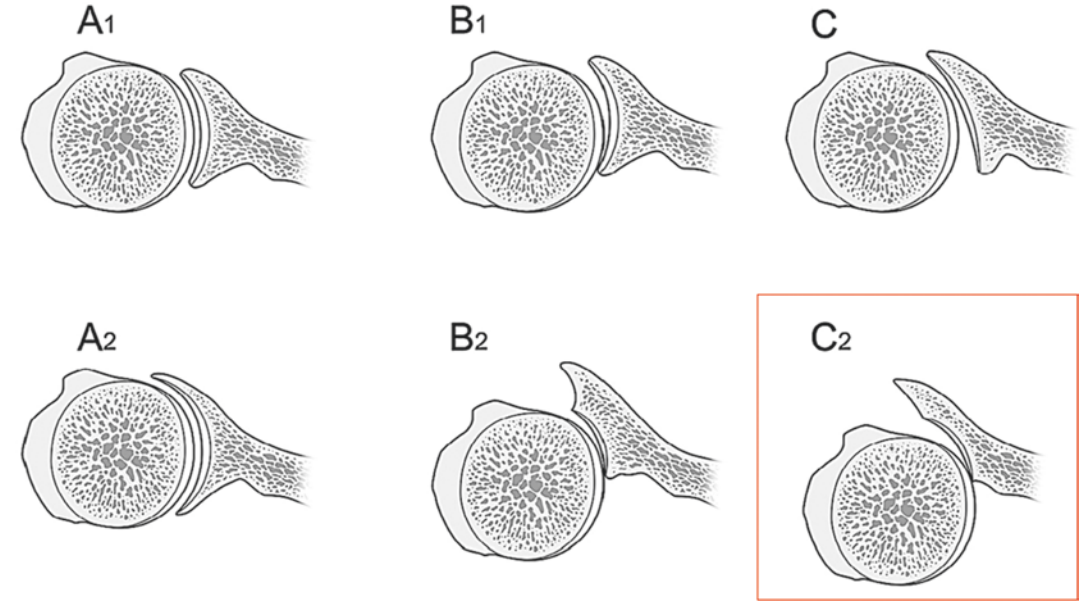

Fig. 47.7 Classification of glenoid version according to Walch et al. [20] modified by Davis et al. [22]

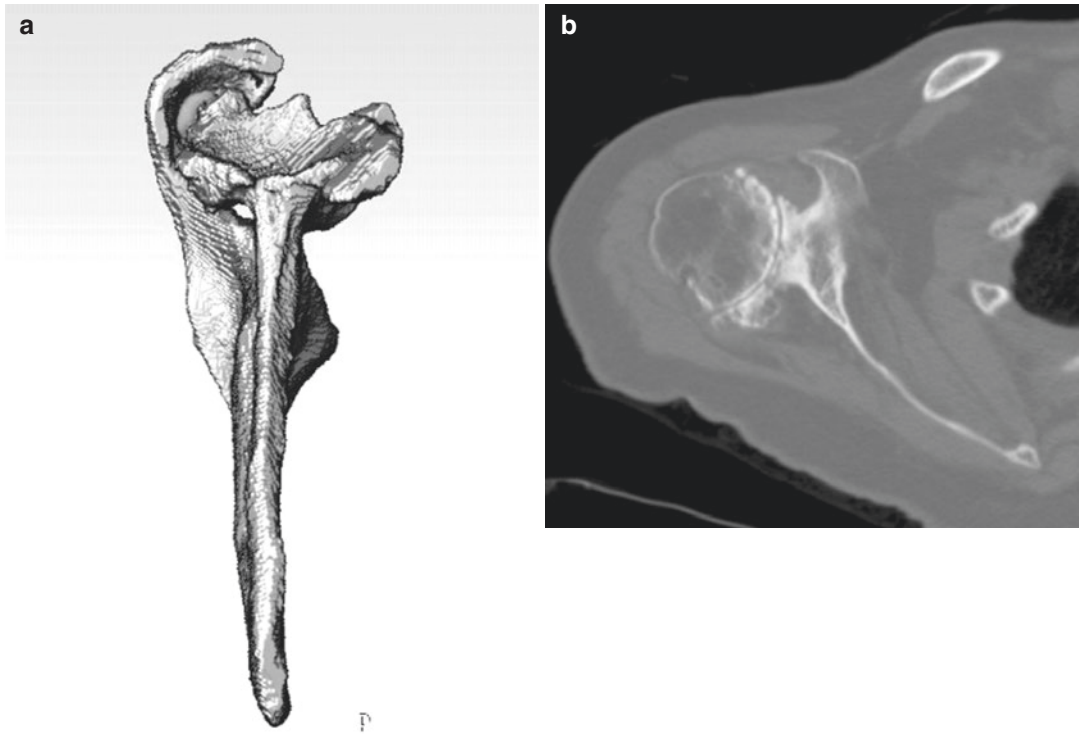

Fig. 47.8 3D CT reconstructions (**a**) are more reliable than 2D CT reconstructions (**b**) in estimating the true glenoid version

to have a reproducible triangular morphology, defined by the endosteal surfaces of the vault. This technique has been first applied to the contralateral, normal glenoid as a template for initial model orientation [27], but subsequently it has been shown that when placed in the best-fit position, the vault model could be used to estimate the physiologic glenoid version in an individual with severe glenoid disease, independent of knowledge of the contralateral glenoid version [28, 29]. Besides the glenoid vault model, several commercial software able to quantify volume, severity, and morphology of glenoid bone loss, with or without the assistance of patient-specific instrumentation (PSI), have been recently developed in order to improve surgeon's ability to place the glenoid implant in the desired location or to understand preoperatively when a standard implant cannot be used [30–33].

47.5 Addressing Glenoid Wear in CTA

Managing severe glenoid bone loss in CTA poses a unique surgical challenge. Historically, these patients were treated with hemiarthroplasty avoiding glenoid implantation. However, clinical studies showed uncertain pain relief and poor functional outcomes [34, 35]. Therefore, up to now, RSA is the best and only treatment option in Stage IVb and V CTA according to Hamada's classification [3]. Shoulder arthroplasty is one of the fastest-growing fields in orthopedic surgery. The goal of glenoid implantation is to correct the glenoid version and use the glenoid vault anatomy to maximize fixation and minimize medialization [29]. Based on size and morphology of glenoid wear, different strategies have been developed.

47.5.1 Asymmetric Reaming

Eccentric reaming prior to glenoid component insertion is a common technique used to improve excessive glenoid retroversion. From a technical standpoint, it is quite easy to perform, requiring only attention to the direction of the reamer in order to avoid worsening of the defect. Cannulated reaming systems allow placement of a guide pin to assess planned version correction before reaming.

Indeed, it has been shown that aggressive reaming can reduce the subchondral bone available for implant support, medialize the joint line, and allow cortical perforation of the polyethylene implant [36]. Studies that have attempted to define the limits of eccentric reaming in order to minimize the removal of subchondral bone while maximizing version correction showed that correction of 10° resulted in a significant decrease in anteroposterior glenoid diameter and correction of 15° of retroversion led to either implant peg penetration or inadequate bone support, which means high risk of implant loosening [37, 38]. Although biomechanical studies showed no micromotion when at least 50% of the baseplate is supported by glenoid bone [39, 40], based on clinical studies, it is safer to limit eccentric reaming to mild defects with no more than 10–15° of glenoid retroversion [41].

47.5.2 Bone Grafting

Bone grafting provides a biologic solution in cases of severe bone loss that do not guarantee secure seating of a glenoid component and that are not amenable to adequate correction of glenoid version by standard methods, such as asymmetric reaming or small changes in glenoid or humeral component version.

Indications for bone grafting, based on the previously described radiological features, can be summarized as follows:

- >15° of retroversion (B2-B3-C-C2 glenoid) [21, 22].
- Superior tilt (E3 glenoid) [14].
- Excessive medialization (Type 2–3) [15].
- Loss of depth: 10–15 mm (axial CT) [33].

Basing treatment on bone loss classifications allows meaningful evaluation of surgical options [42].

Theoretically, advantages of bone grafting in the setting of glenoid wear include preservation of available glenoid bone stock, maintenance of a quite normal joint line that avoids altered joint kinematics secondary to shortening of the glenoid vault, and a permanent restorative solution by biological osseous integration. On the other hand, concerns have also been raised, due to the risk of nonunion, resorption, fixation failure, or subsidence [41, 43]. Moreover, differently from an eccentric reaming, bone grafting is a technically demanding procedure.

Multiple graft sources have been proposed, including humeral head autograft [44, 45], iliac crest autograft [42, 46], cancellous autograft [47, 48], cancellous allograft [49], femoral neck allograft [47], and femoral head allograft [50, 51] (Fig. 47.9).

In 2011, Boileau et al. [44] popularized a standardized technique, which required a specific instrumentation for graft harvesting, preparation, and implantation, called “bony increased offset reverse shoulder arthroplasty” (BIO-RSA; Wright Med Group, Memphis, TN, USA). Recently, the BIO-RSA technique has been updated by introducing the angled BIO-RSA, an asymmetric BIO-RSA which adds more flexibility in managing multiplanar defects by using a trapezoidal bone graft in order to correct not only version and medialization but also the superior tilt [52], based on the assumption that uncorrected superior glenoid erosion (E2, E3 glenoid) [14] can lead to superior tilt of the baseplate which can result in increased scapular impingement, instability, inferior scapular notching, and medial polyethylene wear [53, 54]. At the same time, several companies designed their own instrumentation for symmetrical and asymmetrical bone grafting (Fig. 47.10).

Bateman et al. [47], in order to maximize integration and stability, also proposed a hybrid graft glenoid reconstruction by using a peripherally seated cortical femoral neck allograft acting as a sleeve bushing to provide a stable ring under compression in which to house impacted cancel-

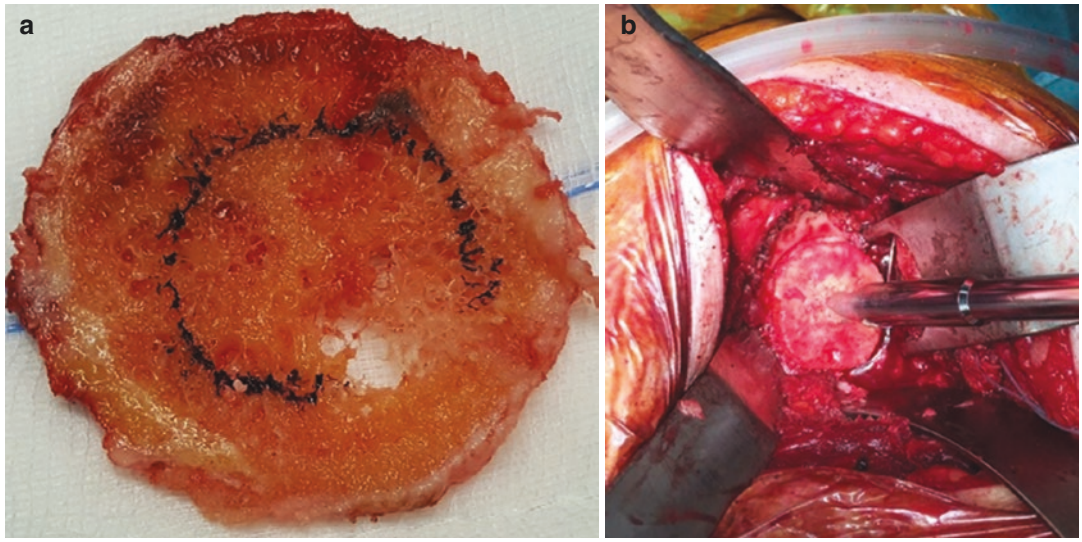

Fig. 47.9 Impaction graft of autologous humeral head to treat a A2 glenoid (**a**, **b**)

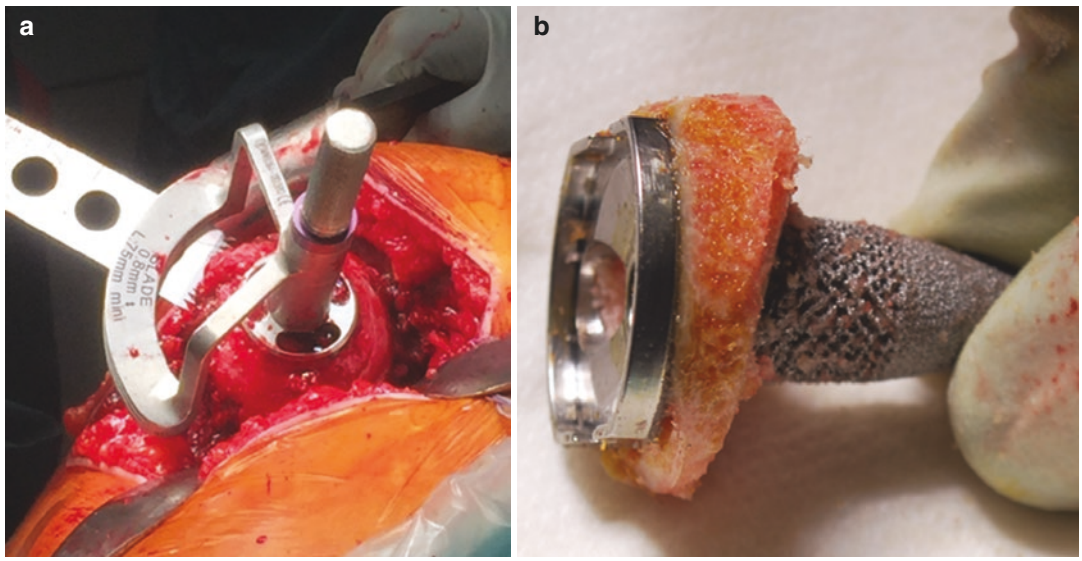

Fig. 47.10 Instrumentation for bone grafting from the humeral head (**a**). Asymmetrical bone graft (**b**)

lous autograft centrally for early incorporation and ingrowth.

Applying the principles of BIO-RSA (symmetric and asymmetric), it is authors' preference to use distal tibial allograft as a bone graft source, when the autologous humeral head is not available (e.g., osteoporosis, humeral head collapse, revision cases) (Fig. 47.11). Distal tibial allograft has been recently introduced as a viable treatment option for glenoid bone loss in anterior and posterior shoulder instability [55, 56]. Main advantages over other bone graft are mainly related to the radius of curvature of the lateral aspect of the distal tibia, which resembles that of the native glenoid, thus providing a more anatomical reconstruction. Besides, the graft contains a cartilaginous layer, so the subchondral bone is thick and dense and acts as adequate support for baseplate fixation [57].

Unfortunately, results of glenoid bone grafting in RSA remain controversial. A high rate of graft

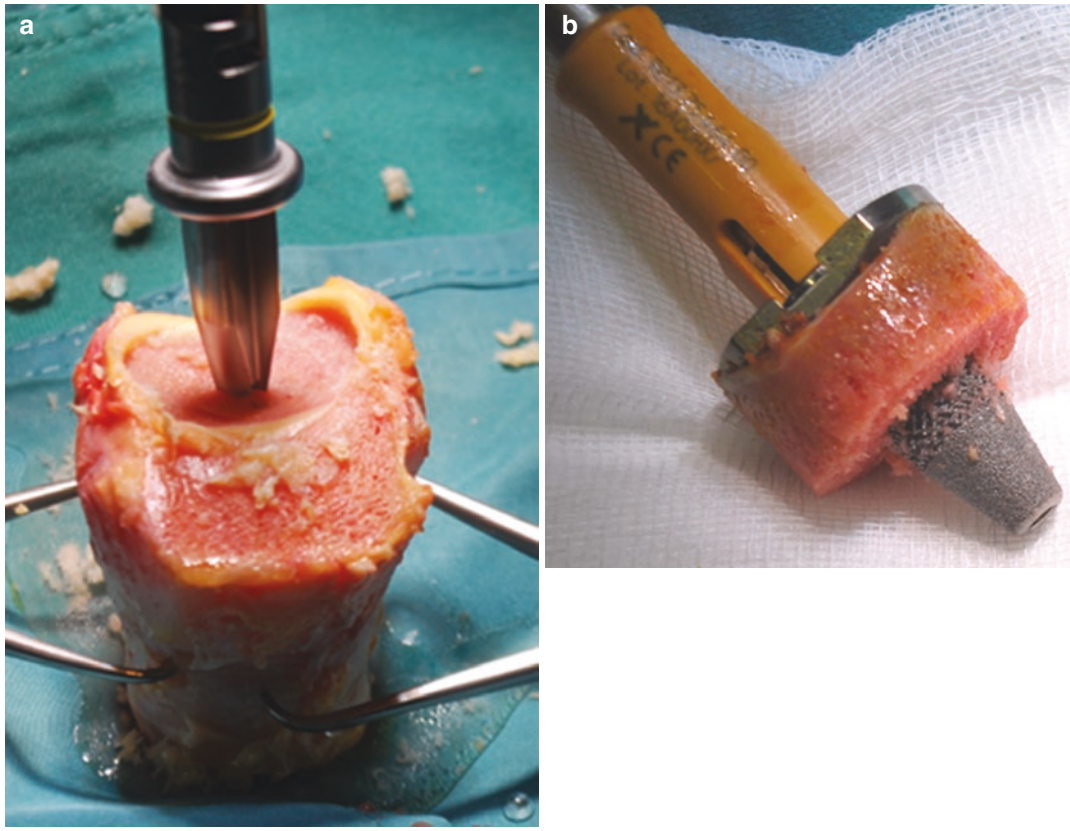

Fig. 47.11 Distal tibia allograft for treating large glenoid bone defects (**a**, **b**)

subsidence, graft resorption, and instability has resulted in early glenoid component loosening and early failure in some studies [58, 59], while some others showed encouraging results with rates of graft incorporation ranging between 76% and 98% [44, 48]. Also, optimal graft source and technique for placement and stabilization remain controversial because of comparison of cohort studies including different grafting techniques and implants and with uncontrolled confounding patient-related variables.

47.5.3 Augmented Baseplate

New prosthetic solutions to glenoid bone loss have been proposed to overcome concerns raised about previously described options. However, similarly to bone grafting, augmented glenoid baseplate implantation is a technically demanding procedure that requires precise creation of a glenoid bone bed to seat the augmented component in order to avoid micromotion and risk of loosening [41].

Literature is still lacking on this topic, even if encouraging results in very small case series have been reported [60–63]. Different designs with various degrees of version and thickness have been described, such as wedged glenoid, usable with or without bone grafting, which allows multiplanar correction of glenoid wear [63], or a customized porous tantalum augment in order to improve lateralization [60] (Fig. 47.12).

Finite element studies comparing bone grafting versus augmented baseplate implantation showed that bony lateralization increases stress and displacement to a greater degree than prosthetic lateralization [64, 65]. Particularly, Denard et al. [64] showed that bony lateralization is not advisable if more than 5 mm are required. Clinical studies are needed.

Fig. 47.12 Augmented baseplate design with symmetrical porous tantalum augment

Fig. 47.13 Custom-made implants should be considered a salvage option in CTA or in revision after failed RSA with severe bone loss

47.5.4 Custom-Made Implants

Custom-made implants should be considered a salvage option in CTA or in revision after failed RSA with severe bone loss (Fig. 47.13).

First examples were CAD/CAM (computer-assisted design/computer-assisted manufacture) shoulder replacement resembling a total hip prosthesis [66–68]. Subsequently, more suitable designs, helped by PSI technology, have been proposed to treat massive glenoid defects [69].

However, further studies are needed before drawing any conclusion on actual results.

References

1. Neer CS, Craig EV, Fukuda H. Cuff-tear arthropathy. J Bone Joint Surg Am. 1983;65:1232–44.
2. Jensen KL, Williams GR, Russell IJ, Rockwood CA. Rotator cuff tear arthropathy. J Bone Joint Surg Am. 1999;81:1312–24.
3. Hamada K, Fukuda H, Mikasa M, Kobayashi Y. Roentgenographic findings in massive rotator cuff tears. A long-term observation. Clin Orthop. 1990;254:92–6.
4. Visotsky JL, Basamania C, Seebauer L, et al. Cuff tear arthropathy: pathogenesis, classification, and algorithm for treatment. J Bone Joint Surg Am. 2004;86-A(Suppl 2):35–40.
5. Rugg CM, Gallo RA, Craig EV, Feeley BT. The pathogenesis and management of cuff tear arthropathy. J Shoulder Elb Surg. 2018;27:2271–83. https://doi.org/10.1016/j.jse.2018.07.020.
6. Aumiller WD, Kleuser TM. Diagnosis and treatment of cuff tear arthropathy. JAAPA. 2015;28:33–8. https://doi.org/10.1097/01.JAA.0000469435.44701.ce.
7. Gumina S, Castagna A, Candela V, et al. Aetiopathogenesis of cuff-tear arthropathy: could juvenile joint laxity be considered a predisposing factor? Int Orthop. 2018;42:1113–7. https://doi.org/10.1007/s00264-017-3718-5.
8. Halverson PB, Cheung HS, McCarty DJ, et al. "Milwaukee shoulder"—association of microspheroids containing hydroxyapatite crystals, active collagenase, and neutral protease with rotator cuff defects. II. Synovial fluid studies. Arthritis Rheum. 1981;24:474–83.
9. McCarty DJ. Milwaukee shoulder syndrome. Trans Am Clin Climatol Assoc. 1991;102:271–83.. discussion 283–4
10. Burkhart SS, Nottage WM, Ogilvie-Harris DJ, et al. Partial repair of irreparable rotator cuff tears. Arthroscopy. 1994;10:363–70.
11. Nam D, Maak TG, Raphael BS, et al. Rotator cuff tear arthropathy: evaluation, diagnosis, and treatment: AAOS exhibit selection. J Bone Joint Surg Am. 2012;94:e34. https://doi.org/10.2106/JBJS.K.00746.
12. Nyffeler RW, Jost B, Pfirrmann CWA, Gerber C. Measurement of glenoid version: conventional radiographs versus computed tomography scans. J Shoulder Elb Surg. 2003;12:493–6. https://doi.org/10.1016/S1058274603001812.
13. Habermeyer P, Magosch P, Luz V, Lichtenberg S. Three-dimensional glenoid deformity in patients with osteoarthritis: a radiographic analysis. J Bone Joint Surg Am. 2006;88:1301–7. https://doi.org/10.2106/JBJS.E.00622.

14. Sirveaux F, Favard L, Oudet D, et al. Grammont inverted total shoulder arthroplasty in the treatment of glenohumeral osteoarthritis with massive rupture of the cuff. Results of a multicentre study of 80 shoulders. J Bone Joint Surg Br. 2004;86:388–95.
15. Kocsis G, Thyagarajan DS, Fairbairn KJ, Wallace WA. A new classification of glenoid bone loss to help plan the implantation of a glenoid component before revision arthroplasty of the shoulder. Bone Joint J. 2016;98-B:374–80. https://doi.org/10.1302/0301-620X.98B3.36664.
16. Churchill RS, Brems JJ, Kotschi H. Glenoid size, inclination, and version: an anatomic study. J Shoulder Elb Surg. 2001;10:327–32. https://doi.org/10.1067/mse.2001.115269.
17. Walker KE, Simcock XC, Jun BJ, et al. Progression of glenoid morphology in glenohumeral osteoarthritis. J Bone Joint Surg Am. 2018;100:49–56. https://doi.org/10.2106/JBJS.17.00064.
18. Donohue KW, Ricchetti ET, Ho JC, Iannotti JP. The association between rotator cuff muscle fatty infiltration and glenoid morphology in glenohumeral osteoarthritis. J Bone Joint Surg Am. 2018;100:381–7. https://doi.org/10.2106/JBJS.17.00232.
19. Scalise JJ, Codsi MJ, Bryan J, et al. The influence of three-dimensional computed tomography images of the shoulder in preoperative planning for total shoulder arthroplasty. J Bone Joint Surg Am. 2008;90:2438–45. https://doi.org/10.2106/JBJS.G.01341.
20. Walch G, Badet R, Boulahia A, Khoury A. Morphologic study of the glenoid in primary glenohumeral osteoarthritis. J Arthroplast. 1999;14:756–60.
21. Bercik MJ, Kruse K, Yalizis M, et al. A modification to the Walch classification of the glenoid in primary glenohumeral osteoarthritis using three-dimensional imaging. J Shoulder Elb Surg. 2016;25:1601–6. https://doi.org/10.1016/j.jse.2016.03.010.
22. Davis DE, Acevedo D, Williams A, Williams G. Total shoulder arthroplasty using an inlay mini-glenoid component for glenoid deficiency: a 2-year follow-up of 9 shoulders in 7 patients. J Shoulder Elb Surg. 2016;25:1354–61. https://doi.org/10.1016/j.jse.2015.12.010.
23. Budge MD, Lewis GS, Schaefer E, et al. Comparison of standard two-dimensional and three-dimensional corrected glenoid version measurements. J Shoulder Elb Surg. 2011;20:577–83. https://doi.org/10.1016/j.jse.2010.11.003.
24. Kwon YW, Powell KA, Yum JK, et al. Use of three-dimensional computed tomography for the analysis of the glenoid anatomy. J Shoulder Elb Surg. 2005;14:85–90. https://doi.org/10.1016/j.jse.2004.04.011.
25. Daggett M, Werner B, Gauci MO, et al. Comparison of glenoid inclination angle using different clinical imaging modalities. J Shoulder Elb Surg. 2016;25:180–5. https://doi.org/10.1016/j.jse.2015.07.001.
26. Werner BS, Hudek R, Burkhart KJ, Gohlke F. The influence of three-dimensional planning on decision-making in total shoulder arthroplasty. J Shoulder Elb Surg. 2017;26:1477–83. https://doi.org/10.1016/j.jse.2017.01.006.
27. Codsi MJ, Bennetts C, Gordiev K, et al. Normal glenoid vault anatomy and validation of a novel glenoid implant shape. J Shoulder Elb Surg. 2008;17:471–8. https://doi.org/10.1016/j.jse.2007.08.010.
28. Scalise JJ, Codsi MJ, Bryan J, Iannotti JP. The three-dimensional glenoid vault model can estimate normal glenoid version in osteoarthritis. J Shoulder Elb Surg. 2008;17:487–91. https://doi.org/10.1016/j.jse.2007.09.006.
29. Ganapathi A, McCarron JA, Chen X, Iannotti JP. Predicting normal glenoid version from the pathologic scapula: a comparison of 4 methods in 2- and 3-dimensional models. J Shoulder Elb Surg. 2011;20:234–44. https://doi.org/10.1016/j.jse.2010.05.024.
30. Iannotti JP, Weiner S, Rodriguez E, et al. Three-dimensional imaging and templating improve glenoid implant positioning. J Bone Joint Surg Am. 2015;97:651–8. https://doi.org/10.2106/JBJS.N.00493.
31. Lombardo DJ, Khan J, Prey B, et al. Quantitative assessment and characterization of glenoid bone loss in a spectrum of patients with glenohumeral osteoarthritis. Musculoskelet Surg. 2016;100:179–85. https://doi.org/10.1007/s12306-016-0406-3.
32. Nowak DD, Bahu MJ, Gardner TR, et al. Simulation of surgical glenoid resurfacing using three-dimensional computed tomography of the arthritic glenohumeral joint: the amount of glenoid retroversion that can be corrected. J Shoulder Elb Surg. 2009;18:680–8. https://doi.org/10.1016/j.jse.2009.03.019.
33. Sabesan V, Callanan M, Sharma V, Iannotti JP. Correction of acquired glenoid bone loss in osteoarthritis with a standard versus an augmented glenoid component. J Shoulder Elb Surg. 2014;23:964–73. https://doi.org/10.1016/j.jse.2013.09.019.
34. Lynch JR, Clinton JM, Dewing CB, et al. Treatment of osseous defects associated with anterior shoulder instability. J Shoulder Elb Surg. 2009;18:317–28. https://doi.org/10.1016/j.jse.2008.10.013.
35. Levine WN, Djurasovic M, Glasson JM, et al. Hemiarthroplasty for glenohumeral osteoarthritis: results correlated to degree of glenoid wear. J Shoulder Elb Surg. 1997;6:449–54.
36. Walch G, Young AA, Boileau P, et al. Patterns of loosening of polyethylene keeled glenoid components after shoulder arthroplasty for primary osteoarthritis: results of a multicenter study with more than five years of follow-up. J Bone Joint Surg Am. 2012;94:145–50. https://doi.org/10.2106/JBJS.J.00699.
37. Clavert P, Millett PJ, Warner JJP. Glenoid resurfacing: what are the limits to asymmetric reaming for posterior erosion? J Shoulder Elb Surg. 2007;16:843–8. https://doi.org/10.1016/j.jse.2007.03.015.
38. Gillespie R, Lyons R, Lazarus M. Eccentric reaming in total shoulder arthroplasty: a cadaveric study. Orthopedics. 2009;32:21.

39. Formaini NT, Everding NG, Levy JC, et al. The effect of glenoid bone loss on reverse shoulder arthroplasty baseplate fixation. J Shoulder Elb Surg. 2015;24:e312–9. https://doi.org/10.1016/j.jse.2015.05.045.
40. Martin EJ, Duquin TR, Ehrensberger MT. Reverse total shoulder glenoid baseplate stability with superior glenoid bone loss. J Shoulder Elb Surg. 2017;26:1748–55. https://doi.org/10.1016/j.jse.2017.04.020.
41. Stephens SP, Paisley KC, Jeng J, et al. Shoulder arthroplasty in the presence of posterior glenoid bone loss. J Bone Joint Surg Am. 2015;97:251–9. https://doi.org/10.2106/JBJS.N.00566.
42. Norris TR. Glenoid bone loss in reverse shoulder arthroplasty treated with bone graft techniques. Am J Orthop (Belle Mead NJ). 2018;47:PMID: 29611849. https://doi.org/10.12788/ajo.2018.0016.
43. Sears BW, Johnston PS, Ramsey ML, Williams GR. Glenoid bone loss in primary total shoulder arthroplasty: evaluation and management. J Am Acad Orthop Surg. 2012;20:604–13. https://doi.org/10.5435/JAAOS-20-09-604.
44. Boileau P, Moineau G, Roussanne Y, O'Shea K. Bony increased-offset reversed shoulder arthroplasty: minimizing scapular impingement while maximizing glenoid fixation. Clin Orthop. 2011;469:2558–67. https://doi.org/10.1007/s11999-011-1775-4.
45. Neyton L, Boileau P, Nové-Josserand L, et al. Glenoid bone grafting with a reverse design prosthesis. J Shoulder Elb Surg. 2007;16:S71–8. https://doi.org/10.1016/j.jse.2006.02.002.
46. Hill JM, Norris TR. Long-term results of total shoulder arthroplasty following bone-grafting of the glenoid. J Bone Joint Surg Am. 2001;83-A:877–83.
47. Bateman E, Donald SM. Reconstruction of massive uncontained glenoid defects using a combined autograft-allograft construct with reverse shoulder arthroplasty: preliminary results. J Shoulder Elb Surg. 2012;21:925–34. https://doi.org/10.1016/j.jse.2011.07.009.
48. Melis B, Bonnevialle N, Neyton L, et al. Glenoid loosening and failure in anatomical total shoulder arthroplasty: is revision with a reverse shoulder arthroplasty a reliable option? J Shoulder Elb Surg. 2012;21:342–9. https://doi.org/10.1016/j.jse.2011.05.021.
49. Elhassan B, Christensen TJ, Wagner ER. Feasibility of latissimus and teres major transfer to reconstruct irreparable subscapularis tendon tear: an anatomic study. J Shoulder Elb Surg. 2014;23:492–9. https://doi.org/10.1016/j.jse.2013.07.046.
50. De Biase CF, Ziveri G, De Caro F, et al. Reverse shoulder arthroplasty using a "L" shaped allograft for glenoid reconstruction in a patient with massive glenoid bone loss: case report. Eur Rev Med Pharmacol Sci. 2014;18:44–9.
51. Klein SM, Dunning P, Mulieri P, et al. Effects of acquired glenoid bone defects on surgical technique and clinical outcomes in reverse shoulder arthroplasty. J Bone Joint Surg Am. 2010;92:1144–54. https://doi.org/10.2106/JBJS.I.00778.
52. Boileau P, Morin-Salvo N, Gauci M-O, et al. Angled BIO-RSA (bony-increased offset-reverse shoulder arthroplasty): a solution for the management of glenoid bone loss and erosion. J Shoulder Elb Surg. 2017;26:2133–42. https://doi.org/10.1016/j.jse.2017.05.024.
53. Laver L, Garrigues GE. Avoiding superior tilt in reverse shoulder arthroplasty: a review of the literature and technical recommendations. J Shoulder Elb Surg. 2014;23:1582–90. https://doi.org/10.1016/j.jse.2014.06.029.
54. Hettrich CM, Permeswaran VN, Goetz JE, Anderson DD. Mechanical tradeoffs associated with glenosphere lateralization in reverse shoulder arthroplasty. J Shoulder Elb Surg. 2015;24:1774–81. https://doi.org/10.1016/j.jse.2015.06.011.
55. Frank RM, Romeo AA, Richardson C, et al. Outcomes of latarjet versus distal tibia allograft for anterior shoulder instability repair: a matched cohort analysis. Am J Sports Med. 2018;46:1030–8. https://doi.org/10.1177/0363546517744203.
56. Frank RM, Shin J, Saccomanno MF, et al. Comparison of glenohumeral contact pressures and contact areas after posterior glenoid reconstruction with an iliac crest bone graft or distal tibial osteochondral allograft. Am J Sports Med. 2014;42:2574–82. https://doi.org/10.1177/0363546514545860.
57. Rabinowitz J, Friedman R, Eichinger JK. Management of glenoid bone loss with anterior shoulder instability: indications and outcomes. Curr Rev Musculoskelet Med. 2017;10:452–62. https://doi.org/10.1007/s12178-017-9439-y.
58. Klika BJ, Wooten CW, Sperling JW, et al. Structural bone grafting for glenoid deficiency in primary total shoulder arthroplasty. J Shoulder Elb Surg. 2014;23:1066–72. https://doi.org/10.1016/j.jse.2013.09.017.
59. Scalise JJ, Iannotti JP. Bone grafting severe glenoid defects in revision shoulder arthroplasty. Clin Orthop. 2008;466:139–45. https://doi.org/10.1007/s11999-007-0065-7.
60. Ivaldo N, Mangano T, Caione G, et al. Customized tantalum-augmented reverse shoulder arthroplasty for glenoid bone defect and excessive medialization: description of the technique. Musculoskelet Surg. 2016;100:13–8. https://doi.org/10.1007/s12306-016-0404-5.
61. Jones RB, Wright TW, Roche CP. Bone grafting the glenoid versus use of augmented glenoid baseplates with reverse shoulder arthroplasty. Bull Hosp Jt Dis. 2015;2013(73 Suppl 1):S129–35.
62. Wright TW, Roche CP, Wright L, et al. Reverse shoulder arthroplasty augments for glenoid wear. Comparison of posterior augments to superior augments. Bull Hosp Joint Dis. 2015;2013(73 Suppl 1):S124–8.

63. Jones RB, Wright TW, Zuckerman JD. Reverse total shoulder arthroplasty with structural bone grafting of large glenoid defects. J Shoulder Elb Surg. 2016;25:1425–32. https://doi.org/10.1016/j.jse.2016.01.016.
64. Denard PJ, Lederman E, Parsons BO, Romeo AA. Finite element analysis of glenoid-sided lateralization in reverse shoulder arthroplasty. J Orthop Res. 2017;35:1548–55. https://doi.org/10.1002/jor.23394.
65. Yang C-C, Lu C-L, Wu C-H, et al. Stress analysis of glenoid component in design of reverse shoulder prosthesis using finite element method. J Shoulder Elb Surg. 2013;22:932–9. https://doi.org/10.1016/j.jse.2012.09.001.
66. Jeske H-C, Wambacher M, Dallapozza C, et al. Functional and clinical outcome of total shoulder arthroplasty with oversized glenoid. Arch Orthop Trauma Surg. 2012;132:927–36. https://doi.org/10.1007/s00402-012-1496-5.
67. Uri O, Bayley I, Lambert S. Hip-inspired implant for revision of failed reverse shoulder arthroplasty with severe glenoid bone loss. Improved clinical outcome in 11 patients at 3-year follow-up. Acta Orthop. 2014;85:171–6. https://doi.org/10.3109/17453674.2014.899850.
68. Chammaa R, Uri O, Lambert S. Primary shoulder arthroplasty using a custom-made hip-inspired implant for the treatment of advanced glenohumeral arthritis in the presence of severe glenoid bone loss. J Shoulder Elb Surg. 2017;26:101–7. https://doi.org/10.1016/j.jse.2016.05.027.
69. Dines DM, Gulotta L, Craig EV, Dines JS. Novel solution for massive glenoid defects in shoulder arthroplasty: a patient-specific glenoid vault reconstruction system. Am J Orthop (Belle Mead NJ). 2017;46:104–8.